Measurement of the Heme Affinity for Yeast Dap1p, and Its Importance in Cellular Function †

ARTICLE *in* BIOCHEMISTRY · JANUARY 2008

Impact Factor: 3.02 · DOI: 10.1021/bi7013739 · Source: PubMed

Measurement of the Heme Affinity for Yeast Dap1p, and Its Importance in Cellular Function†

Alisha M. Thompson,‡ Amit R. Reddi,§ Xiaoli Shi,# Robert A. Goldbeck,‡ Pierre Moënne-Loccoz,⊥ Brian R. Gibney,§ and Theodore R. Holman*,‡

Department of Chemistry and Biochemistry, University of California, Santa Cruz, California 95064, Department of Chemistry, Columbia University, 3000 Broadway, MC 3121, New York, New York, 10027, and Department of Environmental and Biomolecular Systems, OGI School of Science and Engineering, Oregon Health and Science University, 20,000 NW Walker Road, Beaverton, Oregon 97006

Received July 11, 2007; Revised Manuscript Received October 5, 2007

ABSTRACT: Current studies on the *Saccharomyces cerevisiae* protein Dap1p have demonstrated a heme-related function within the ergosterol biosynthetic pathway. Here we present data to further the understanding of the role of heme in the proper biological functioning of Dap1p in cellular processes. First, we examined the role of Dap1p in stabilizing the P_{450} enzyme, Erg11p, a key regulatory protein in ergosterol biosynthesis. Our data indicate that the absence of Dap1p does not affect Erg11p mRNA, protein expression levels, or the protein degradation rates in *S. Cerevisaie*. Second, in order to probe the role of heme in the biological functioning of Dap1p, we measured ferric and ferrous heme binding affinities for Dap1p and the mutant $Dap1p^{Y138F}$, as well as equilibrium midpoint reduction potentials of the Fe(III)/Fe(II) couples. Our results show that both wild-type and mutant proteins bind heme in a 1:1 fashion, possessing tight ferric heme affinities, K_D values of 400 pM and 200 nM, respectively, but exhibiting weak ferrous affinities, 2 and 10 μM, respectively. Additionally, the measured reduction potential of Dap1p, which was found to be −307 mV, is similar to that of other monotyrosinate hemoproteins. Although previous reports show the weaker affinity of $Dap1p^{Y138F}$ for ferric heme lowers the production of ergosterol with respect to wild-type Dap1p in *S. pombe*, we find that $Dap1p^{Y138F}$ expression is still sufficient to rescue the growth sensitivity of *dap1*Δ to fluconazole and methyl methanesulfonate in *S. cerevisiae*. Various interpretations of these results are discussed with respect to Dap1p function in the cell.

The yeast protein, Dap1p,[1] belongs to a highly conserved and ubiquitous protein family known as membrane-associated progesterone receptors, MAPRs. One of the first characterized members of this family was found in porcine liver tissues and was identified by its ability to bind progesterone (*1*−*3*). In the same year, the gene for the rat homologue was isolated and characterized as a novel gene induced by 2,3,7,8-tetrachlorodibenzo-*p*-dioxin from rat livers (*4*). Homologous members of this family have subsequently been identified, via sequence alignments, in all eukaryotes, from protozoans to humans. They share a conserved cytochrome b_5 heme binding motif (*5*), although, the protein sequences lack the two histidines required for cytochrome b_5 binding of heme. Nevertheless, within the last 5 years, evidence has been mounting toward a biological role for heme binding to several of the well-characterized MAPRs, including Dap1p (*6*−*10*).

The Dap1p homologue in *S. cerevisiae* was first characterized in a deletion strain, *dap1*Δ, by its sensitivity to methyl methanesulfonate (MMS), a DNA damaging agent, and to fluconazole/itraconazole, Erg11p sterol synthesis inhibitors (*11*). *Dap1*Δ strains were later shown to be rescued from the MMS sensitivity by the presence of hemin in the media, both in growth and sterol production (*8*). Mallory et al. also demonstrated that overexpression of Erg11p in *dap1*Δ decreased sensitivity to itraconazole. Although, *dap1*Δ did not affect mRNA levels of Erg11p, Mallory et al. did report lowered protein levels of Erg11p, suggesting a protein regulatory function for Dap1p, possibly as a heme chaperone (*8*). It was also reported at this time that a Dap1p fusion protein bound heme, although its heme ligation was unknown. The heme binding of Dap1p was further character-

† This research was supported by NIH Grant GM56062-06 (T.R.H.), the Roche Foundation for Anemia Research (T.R.H.), NIH Grant EB02056 (R.A.G.), the National Science Foundation GK-12 Graduate Fellowship (DGE-02-31875) (A.R.R.) and the American Heart Association Grant-in-Aid (0755879T) (B.R.G.).

* To whom correspondence should be addressed. Phone: (831) 459-3871. Fax: (831) 459-2935. E-mail: tholman@chemistry.ucsc.edu.

‡ University of California, Santa Cruz.

§ Columbia University.

⊥ Oregon Health and Science University.

Current address: Department of Radiation Oncology, Stanford University, Palo Alto, CA, 94305.

[1] Abbreviations: Dap1p, wild-type yeast Dap1 protein; $Dap1p^{Y138F}$, Dap1p-Tyr138Phe; $Dap1p^{D91G}$, Dap1p-Asp91Gly; Erg11p, yeast lanosterol 14-α-demethylase protein; Erg11p-HA, yeast lanosterol 14-α-demethylase protein with a hemagglutinin tag on the C-Terminus; *DAP1*, wild-type yeast Dap1 gene; *ERG11*; yeast lanosterol 14-α-demethylase gene; PGRMC1, progesterone receptor membrane component-1 protein; MAPR, membrane-associated progesterone binding protein; IZA, rat inner zone antigen; SD−His, synthetically defined media lacking histidine; PGK, phosphoglycerate kinase; AAA, amino acid analysis; ICP-MS, inductively coupled plasma mass spectrometry; MMS, methyl methanesulfonate; Mb, myoglobin; apoMb, apomyoglobin; HSM, horse skeletal muscle; TBP, TATA box binding protein; RR, resonance Raman; SHE, standard hydrogen electrode; GC−MS, gas chromatography mass spectrometry.

10.1021/bi7013739 CCC: $37.00
Published on Web 11/22/2007

ized by our group as a pentacoordinate, ferric heme, with Tyr138 as the axial ligand (*7*). Hughes et al. recently reported that the *S. pombe* Dap1p homologue (which shares 67% homology to *S. cerevisiae* Dap1p) bound Erg11p in a 1:1 ratio and by comparing the sterol profiles of wild-type, *dap1*Δ, and Dap1p^{Y138F} found that heme binding by Dap1p was important for maintaining proper sterol production (*9*). Hughes et al. also demonstrated that the protein level of the human homologue of Erg11p, Cyp51A1, was not affected by the loss of the human homologue of Dap1p, PGRMC1, supporting their hypothesis that MAPRs activate P_{450} cytochromes through a protein−protein interaction and not by chaperoning the heme, contrary to past hypotheses (*6*−*8*). For these reasons, we set out in this study to further characterize the cellular and biochemical properties of the *S. cerevisiae* Dap1p homologue in an attempt to understand its role in yeast biology in more detail.

MATERIALS AND METHODS

Source of Materials. Restriction endonucleases were obtained from New England BioLabs (Beverly, MA). All other chemicals were reagent grade or better and were used without further purification.

Plasmids, Strains, and Growth Conditions. The *E. coli* protein expression plasmids for Dap1p and Dap1p mutants were constructed as previously reported (*7*). Briefly, PCR-amplified *DAP1* gene from yeast genomic DNA was cloned into the *pET28a* vector (Novagen) generating the *pET28a_DAP1* plasmid. All mutants were subsequently created by site-directed mutagenesis using a Quikchange kit (Stratagene), and verified by DNA sequencing.

Yeast vector *pRS313_DAP1* containing the native *DAP1* promoter was constructed by PCR amplifying the *DAP1* open reading frame along with 340 bps of promoter sequence and 254 bps of 3′ UTR, cloned into *pCR2.1-TOPO* (Invitrogen) and subcloned into SpeI/Xho I sites of the low-copy vector *pRS313*. Mutants were made by site-directed mutagenesis on the *pRS313_DAP1* plasmid. Wild-type (BY4741, Invitrogen) and isogenic *dap1*Δ (*BY4741-dap1::KanMX*, Invitrogen) strains transformed with *pRS313*, *pRS313_DAP1*, *pRS313_ DAP1^{D91G}*, or *pRS313_ DAP1^{Y138F}* plasmid were used for drug sensitivity studies.

pRS413GAL_ERG11-HA plasmid was created as follows: EcoR I (5′)/Xho I (3′) fragment containing the *ERG11* open reading frame plus 3HA tag right before the stop codon was generated by PCR from genomic DNA of BY4741 strain and cloned into the EcoR I and Xho I sites of *pRS413GAL* vector. BY4741 wild-type and *dap1*Δ strains transformed with *pRS413GAL_ERG11-HA* were used for Erg11p degradation studies.

pRS303_ERG11-HA was created by subcloning ∼1.3 Kb Xba I/Xho I C-terminal fragment of *ERG11* from *pRS413GAL_ERG11-HA* plasmid into a *pRS303* vector. The resulting *pRS303_ERG11-HA* was linearized by cutting with the unique BspM I and transformed into BY4741 wild-type and *dap1*Δ strains to generate strains with HA-tagged Erg11p at the native chromosomal locus. The integration was confirmed by PCR. The above *ERG11-HA*-tagged strains were grown overnight, diluted, grown in SD−His medium for 4 h, and then harvested for qRT-PCR and Western blotting, respectively.

Quantitative RT-PCR. Early log-phase cells, treated with or without 25 μM hemin, were harvested, and the total RNA was extracted by a Qiagen RNeasy mini kit. Contaminating DNA was removed from 16 μL of RNA extract by the addition of 2 μL of 10× reaction buffer and 2 μL of DNase (Promega RQ1 DNase) and incubating for 30 min at 37 °C. Reactions were terminated by adding 2 μL of stop buffer and heating for 10 min at 65 °C. cDNA was synthesized using Applied Biosystem TaqMan reverse transcription kit by the following modified protocol. Each 20 μL of reaction mixture consisted of 2 μL of 10× TaqMan RT buffer, 4.4 μL of 25 mM $MgCl_2$, 4 μL of dNTP mix, 1 μL of random hexamers, 0.4 μL of RNase inhibitor, 0.6 μL of multiscribe reverse transcriptase (50 U/μL), and 7.6 μL of DNase-treated RNA sample (1 μg total RNA). Reactions were incubated at 25 °C for 10 min, 48 °C for 30 min, followed by heat inactivation at 95 °C for 5 min. Prior to quantitative PCR, cDNAs were diluted 1/4 in nuclease-free water.

The following primers were used for real-time PCR analyses.

ERG11(f): 5′ TTCCGTCGGTGAAGAAGTCGATTACG 3′.

ERG11(r): 5′ ACATCTGTGTCTACCACCACCGAAAG 3′.

TBP(f): 5′ CGGTTCGTGTGACGTTAAATTCC 3′.

TBP(r): 5′ GCACAGGGTATATAGCTTCAAAAGC 3′.

PCR reactions consisted of 4 μL of diluted template (cDNA, standard genomic DNA, or water), 20 μL of 2× SybrGreen Taq mix (Applied Biosystems), 300 nM each primer, and nuclease-free water to make a final volume of 40 μL. PCR was carried out using a MJ Research Opticon 2 in duplicate for triplicate cDNA samples and primer sets. The thermocycle profile was as follows: 95 °C for 10 min, 40 cycles of 95 °C for 30 s and 60 °C for 1 min, with a final denaturation cycle to examine the DNA melting curves of the PCR products.

The cycle thresholds ($C(t)$) were calculated for samples and genomic DNA standards. For each transcript, the $C(t)$ value was converted to a nanogram genomic DNA equivalent by comparing the $C(t)$ of an unknown to standard curves prepared from genomic DNA of strain BY4741(1, 0.1, 0.01, 0.001 ng). Slopes for *ERG11* and *TBP* standard curves ranged from 3.3 to 4.3 and were linear with R^2 of 0.999. Expression was calculated by normalizing the nanogram value for *ERG11* to the nanogram value of *TBP*.

Western Blotting (Determination of Protein Half-Life). Wild-type and isogenic *dap1*Δ yeast strains transformed with *pRS413GAL_ERG11-HA* were grown overnight in SD−His medium containing 2% raffinose, inoculated in the same media, and grown for 4 h. Galactose (0.5%) was added to the SD−His media (2% raffinose) to induce Erg11p protein expression. After 4 h of induction, cells were centrifuged and resuspended in SD−His containing 2% glucose to stop the induction. Aliquots at 0, 60, 120, and 240 min, after stopping induction, were removed for immunoblot analysis. Protein extracts, with the same amount of OD_{600} units by the NaOH/β-mercaptoethanol method, were loaded onto 10% SDS−PAGE and separated by electrophoresis. After transferring, the blot was incubated with a primary rabbit anti-HA antibody Y11 (Santa Cruz Biotech.) and HRP-conjugated secondary goat antirabbit IgG (Santa Cruz Biotech.), developed by ECL, and recorded on ECL Hyper film (Amersham).

The same blot was subsequently incubated with a primary mouse antiyeast 3-phosphoglycerate kinase (PGK) monoclonal antibody (Molecular Probes Invitrogen) and an HRP-conjugated secondary goat antimouse IgG (Santa Cruz Biotech.) as a loading control (*12*).

Growth Phenotype in Fluconazole or MMS Media. The early log-phase cells ($OD_{600} = 0.2$) were serially diluted 10-fold with water and spotted into selective SD media containing either fluconazole or MMS. The plates were incubated at 30 °C for 3 days and photographed.

Purification of Proteins. Purification and expression of Dap1p and Dap1p^{Y138F} were from *E. coli* BL21(DE3) cells and have been previously reported (*7*). Briefly, single colonies of freshly transformed cells were grown in LB broth containing 25 μg/mL of kanamycin (FisherBiotech) at 37 °C and 200 rpm until an OD_{600} of 0.6 was attained. Cultures were then induced with 0.5 mM IPTG and grown overnight at 20 °C and 100 rpm. Cell lysates were precipitated with ammonium sulfate, the 10−40% fraction was passed over a methyl hydrophobic interaction column, and the cleanest protein fractions were passed over a size exclusion column. Fractions of greater than 95% purity, as measured by PAGE, were collected, concentrated, and stored at −80 °C in 5% glycerol.

Circular Dichroism. Purified protein samples, 70−90 μM, were measured in a 0.1 mm cuvette on an AVIV model 60DS, from 190 to 240 nm, in 0.5 nm increments. The average of five spectra were integrated, and measurements of percent α-helicity were based on the absorbance at θ_{222} nm and calculated with the equation: $-\theta_{222}/33\,000 = \%$ α-helicity (*13*).

Measurement of Protein and Heme Extinction Coefficients. Heme content was measured by both ICP-MS analysis and pyridine hemochrome method (*7*, *14*). Protein concentrations were measured by amino acid analysis, AAA, (U.C. Davis) and Bradford Assay (BioRad). Myoglobin was used as a standard due to its similarity in size to Dap1p and its heme binding. The protein extinction coefficient was back-calculated from amino acid analysis by the summation of all amino acids measured against an internal standard, norleucine; a molar protein concentration could then be compared to the electronic spectra (http://msf.ucdavis.edu/calculations.html). The contribution of the heme to the UV−vis absorption at 278 nm was measured by titrating heme into Dap1p and relating it to the Soret band.

Heme Reconstitution. A freshly prepared 100× hemin stock solution in 0.1 M NaOH and 50% dimethyl sulfoxide was used to add 1.5−2-fold excess heme to Dap1p and Dap1p^{Y138F} protein solutions. Protein and heme were left overnight to equilibrate and then washed three times with buffer in 10 kDa centricons for removal of unbound heme. Heme concentration was measured by ICP-MS, and protein concentration was determined by UV−vis absorption and Bradford Assay.

Determination of Binding Constants. The heme binding affinity of Dap1p was measured using two competition binding methods. First, direct titration of horse skeletal muscle (HSM) apomyoglobin into as-isolated, ferric Dap1p, with ∼30% heme bound, was used to estimate the ferric heme K_D value of Dap1p. Singular value decomposition of the UV−vis spectra, coupled with fitting to a competition binding model, was used to determine the ferric K_D^{comp} value (*15*). The K_D value of Dap1p was estimated based on the experimentally derived K_D^{comp} value and the K_D value of HSM myoglobin, which was estimated to be similar to the 10 fM ferric heme K_D value of sperm whale myoglobin (calculations and methods outlined in the Supporting Information) (*16*, *17*). Due to the kinetic trapping of ferrous heme by myoglobin and the lack of a measured ferrous heme K_D value, this approach could not be used to determine the ferrous K_D value of Dap1p (*16*, *17*).

In order to determine more accurate ferric and ferrous K_D values for Dap1p, direct competition titration experiments were performed using a synthetic heme protein maquette, $[\Delta 7\text{-His}]_2$, whose ferric and ferrous K_D values are well-described between pH 5.0 and 9.0. At pH 8.0, $[\Delta 7\text{-His}]_2$ possesses a ferric heme K_D value of 160 pM and a ferrous heme K_D value of 40 nM and is kinetically competent for heme transfer experiments (*18*). To obtain the K_D value for the ferric heme state, apo-$[\Delta 7\text{-His}]_2$ was titrated into a solution of 15 μm Dap1p containing 2.8 μM bound heme; this resulted in a shift in the Soret band maximum from 398 to 412 nm. Heme transfer was evidenced by the increase in the intensity of the Soret band at 412 nm which was monitored after an hour equilibration time.

For ferrous heme equilibrium measurements, apo-$[\Delta 7\text{-His}]_2$ was titrated into a solution of 10.6 μM Dap1p containing 2 μM bound heme under anaerobic conditions and maintained under a reducing redox environment with the addition of a slight excess of sodium dithionite. Over the hour equilibration time, the Soret band shifts from 422 to 427 nm, indicative of heme transfer to the synthetic protein. The equilibrium concentrations of holo-Dap1p and holo-$[\Delta 7\text{-His}]_2$ were calculated based on the intensity at 427 nm.

The heme binding stoichiometry and heme affinity of Dap1p^{Y138F} were measured by direct titration of ferric or ferrous heme, the latter under reducing, anaerobic conditions with a slight excess of sodium dithionite. The affinity of Dap1p^{Y138F} for ferric heme was determined by measuring the increase in absorbance at 398 nm and fitting the data to a 1:1 heme/protein binding equilibrium. The affinity of Dap1p^{Y138F} for ferrous heme was measured in an analogous fashion using the increase in absorbance at 422 nm.

Determination of Heme Reduction Potential of Dap1p. Chemical redox titrations were performed in an anaerobic cuvette equipped with a platinum working electrode and a calomel reference electrode at 22 °C (*19*). Ambient potentials (measured against the standard hydrogen electrode) were adjusted by addition of aliquots (<1 μL) of sodium dithionite or potassium ferricyanide. Titrations were performed in 20 mM potassium phosphate, 100 mM KCl, pH 8.0. Electrode−solution mediation was facilitated by the following mediators at 10 μM concentration: methyl viologen, benzyl viologen, anthroquinone-2-sulfonate, anthroquinone-2,6-disulfonate, 2-hydroxy-1,4-naphthoquinone, duroquinone, 5-hydroxy-1,4-naphthoquinone, 1,4-naphthoquinone, phenazine ethosulfate, and phenazine methosulfate. After equilibration at each potential, the optical spectrum was recorded. Heme reduction was followed by the increase in the Soret band absorption (422 nm) relative to a baseline wavelength (750 nm). Spectral intensity was plotted against potential, and the data were fit to a single Nernst equation with $n = 1.0$ (fixed).

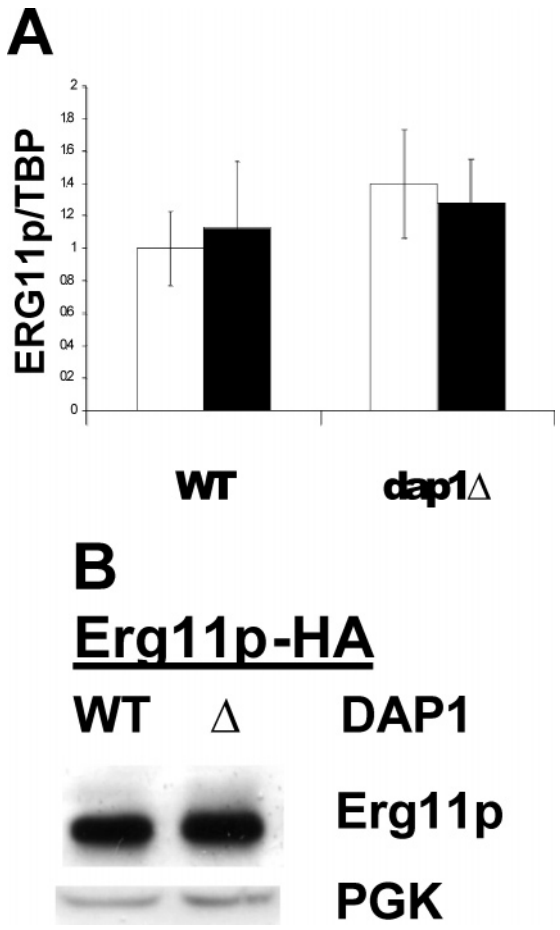

FIGURE 1: (A) Wild-type and *dap1*Δ yeast strains were tested for DNA expression levels of ERG11, as measured by rtPCR (normalized to TBP), while grown with heme (black) and without heme (white). (B) Protein expression levels were measured by Western blot, without the addition of heme.

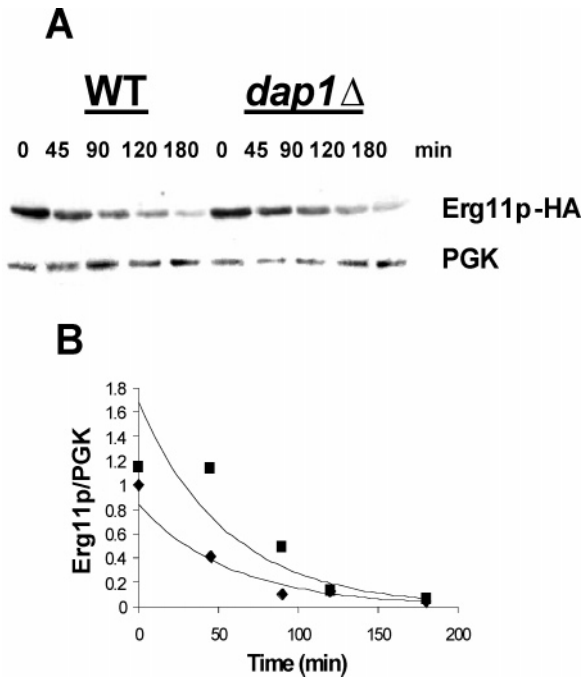

FIGURE 2: Measurement of $t_{1/2}$ of Erg11p in wild-type and *dap1*Δ yeast strains. (A) Protein expression levels of Erg11p and PGK at 0, 45, 90, 120, and 180 min after repression of Erg11p-HA by glucose on the galactose promoter. (B) Calculation of Erg11p degradation rates, relative to PGK(◆) $t_{1/2}$ = 40 min and *dap1*Δ (■) $t_{1/2}$ = 38 min.

RESULTS

mRNA and Protein Expression. mRNA expression levels of *ERG11*, measured by quantitative real-time PCR in ERG11-HA-tagged wild-type and *dap1*Δ strains in triplicate, were found to be unaffected by the absence of Dap1p as previously reported (*8*). Additionally, mRNA expression levels were unaffected by the addition of hemin (Figure 1). Protein levels of Erg11p in the above strains were measured with anti-HA antibody by Western blotting in triplicate and standardized to the house-keeping protein, PGK. Contrary to previously published results for *S. cerevisiae* W303, our results show that Erg11p protein levels were unaffected by the absence of Dap1p in *S. cerevisiae* BY4741 (*8*) (Figure 1). Erg11p-HA protein degradation rates in both wild-type and *dap1*Δ strains transformed with *pRS413GAL-ERG11-HA* plasmid in wild-type and *dap1*Δ strains were monitored by Western blot and standardized to PKG protein levels at 0, 1, 2, and 4 h after the induction/repression. The half-life ($t_{1/2}$) of Erg11p was calculated to be 40 and 38 min in wild-type and *dap1*Δ strains, respectively (Figure 2). Hence, there is no difference between the degradation rate of overexpressed Erg11p in wild-type and that in *dap1*Δ strains.

Sensitivity to Fluconazole and MMS. pRS313, pRS313_DAP1, pRS313_ DAP1^{D91G}, or *pRS313_ DAP1^{Y138F}* plasmids were transformed into wild-type and *dap1*Δ yeast strains and plated on selective media. The *dap1*Δ strain exhibits a growth sensitivity to media containing fluconazole or MMS which can be recovered by native expression of Dap1p but not by Dap1p^{D91G} (data not shown), as previously reported by Mallory et al. (*8*). However, Dap1p^{Y138F} can rescue the growth sensitivity for both fluconazole and MMS to wild-type growth as shown in Figure 3.

Expression and Purification. Dap1p and Dap1p^{Y138F} were both soluble and expressed in *E. coli* at high levels as previously reported (*7*). Despite high levels of expression, attempts to purify a soluble form of untagged or his-tagged Dap1p^{D91G} were unsuccessful due to inclusion bodies. We note that several groups have used Dap1p^{D91G} as a nonfunctional/non-heme binding mutant of Dap1p. Although we agree that this protein appears to be nonfunctional, we caution that the lack of heme binding was observed as a GST fusion protein, which can often solubilize misfolded proteins (*8*, *20*). For this reason we have focused on a Dap1p^{Y138F}, a mutant that demonstrates a lowered heme affinity yet remains soluble as a non-fusion protein.

Circular Dichroism. Circular dichroism was used to measure percent α-helicity to ensure Dap1p and Dap1p^{Y138F} were not grossly misfolded. Dap1p and Dap1p^{Y138F} were found to have 48% and 40% α-helicity, respectively, based on θ_{222} values of 13 252 and 15 858. These percentages are comparable to the ~31% α-helicity derived from the NMR structure of the plant homologue, At2g24940.1 (PDB = 1T0G). The difference may be accounted for by both the smaller size of At2g24940.1 (101 amino acids compared to 152 for Dap1p) and the lack of bound heme from in vitro expression (*21*).

Determination of the Heme Extinction Coefficient. Quantification of heme concentration is typically done by measurement of the ferrous pyridine heme complex (*14*); however, we have found that the standard extinction coef-

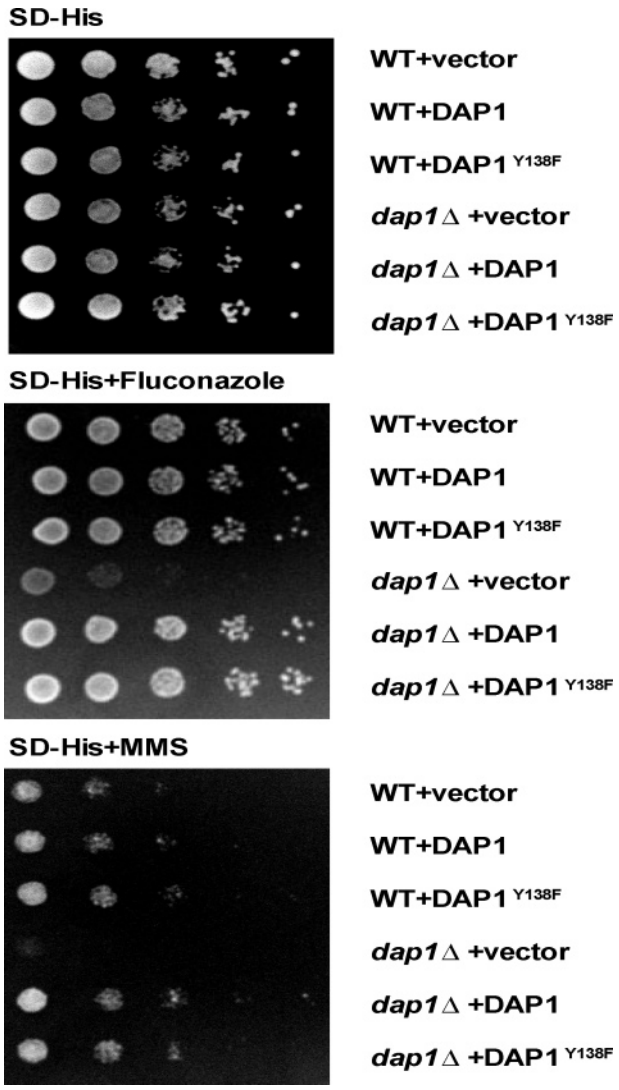

FIGURE 3: Growth of yeast strains wild-type (BY4741) or isogenic *dap1*Δ transformed with pRS313 vector containing either vector only, DAP1, or DAP1^{Y138F}. Cells were serial diluted 1:10 and grown for 3 days at 30 °C.

ficients associated with this method vary with both buffer and pH changes. Instead, we used ICP-MS to determine heme concentration based on iron analysis. From multiple protein preparations, we averaged an extinction coefficient of 96 800 ± 6000 M^{-1} cm^{-1} for Dap1p, which is within error of our previously reported value of 99 000 M^{-1} cm^{-1} (*7*). On the basis of this value, a small feature for Dap1p^{Y138F}, as purified, was noted at 399 nm, corresponding to less than 2% heme bound (Figure 4).

Determination of Protein Extinction Coefficient. The protein extinction coefficient for Dap1p^{Y138F} was measured by both amino acid analysis and the Bradford assay. The average ϵ_{278} for Dap1p ^{Y138F} (<2% heme bound) was measured as 17 000 ± 3500 M^{-1} cm^{-1}, which is within the range of the predicted extinction coefficient of 15 500 M^{-1} cm^{-1} (ExPASy ProtParam tool). Determination of the ϵ_{278} for wild-type Dap1p is complicated by the additional heme absorption at 278 nm. To account for this, we assumed a similar extinction coefficient for the wild-type as that of the mutant Dap1p^{Y138F} (which is also similar to the predicted value of 17 000 M^{-1} cm^{-1}, ExPASy ProtParam tool) and solved for the additional heme extinction coefficient at 278 nm. Based on a titration of heme into a solution of Dap1p, we compared the change at 399 and 278 nm, and using the heme extinction coefficient of 96 800 ± 6000 M^{-1} cm^{-1}, found the heme extinction coefficient at 278 nm to be approximately 22 500 ± 3770 M^{-1} cm^{-1}.

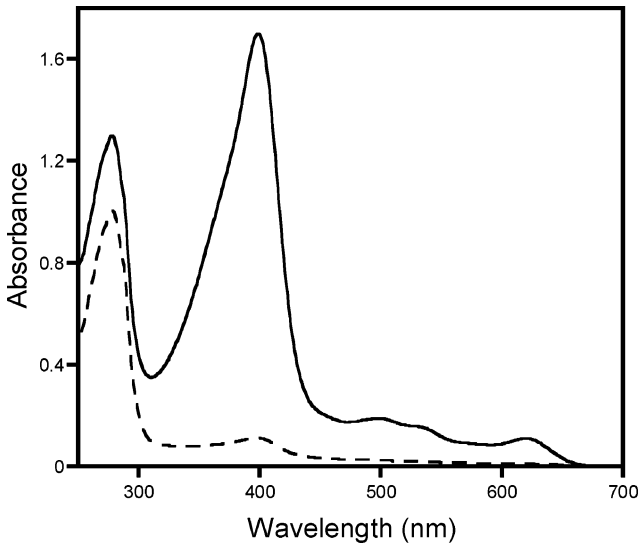

FIGURE 4: Representative UV−vis spectra of 1 mg/mL samples Dap1p (—) (as purified with ∼20% heme bound) and Dap1p^{Y138F} (− − −) (as purified with <2% heme bound).

Heme Binding Constants. Removal of heme from Dap1p was hampered by the fact that standard methods of heme extraction denatured the protein (*22*, *23*). Therefore to measure the K_D, we switched to a competitive binding method using HSM apomyoglobin and a 30% heme-loaded Dap1p sample. This method was used to determine an initial ferric heme dissociation constant of approximately 100 fM for Dap1p, assuming the HSM myoglobin has the same K_D value as that of sperm whale myoglobin, i.e., 10 fM (Supporting Information, Figure S1) (*16*, *17*).

In order to obtain more accurate K_D values in both oxidation states, we utilized the synthetic heme protein maquette, $[\Delta 7\text{-His}]_2$, which has well-determined K_D values in both the ferric and ferrous heme states (*24*). As previously reported, $[\Delta 7\text{-His}]_2$ has a ferric K_D value 160 pM and a ferrous heme K_D value 40 nM at pH 8.0 (*18*). Upon titration of apo-$[\Delta 7\text{-His}]_2$ to a solution of as-isolated Dap1p in the ferric and ferrous states, K_{comp} values are measured as 2.5 ± 1.0 and 35 ± 15, respectively, and with 1:1 heme to protein ratios in both cases. The ferric heme dissociation constant value for Dap1p was then calculated to be 400 ± 200 pM, and the ferrous dissociation constant value is 2 ± 1 μM (Figure 5).

For the mutant Dap1p^{Y138F}, direct titration of heme was possible due to the low initial concentration of heme (<2%) and a weaker affinity for the heme. A protein-to-heme binding ratio of 1:1 is observed by direct titration, and ferric and ferrous heme dissociation constants for Dap1p^{Y138F} were measured as 200 ± 100 nM and 10 ± 5 μM, respectively (Figure 6).

Electrochemistry of Dap1p. Figure 7 shows the electrochemistry of wild-type Dap1p as evaluated using UV−vis spectroelectrochemistry. The change in Soret band absorption upon reduction to ferrous heme was fit to an equilibrium midpoint reduction potential of −307 mV versus SHE. This

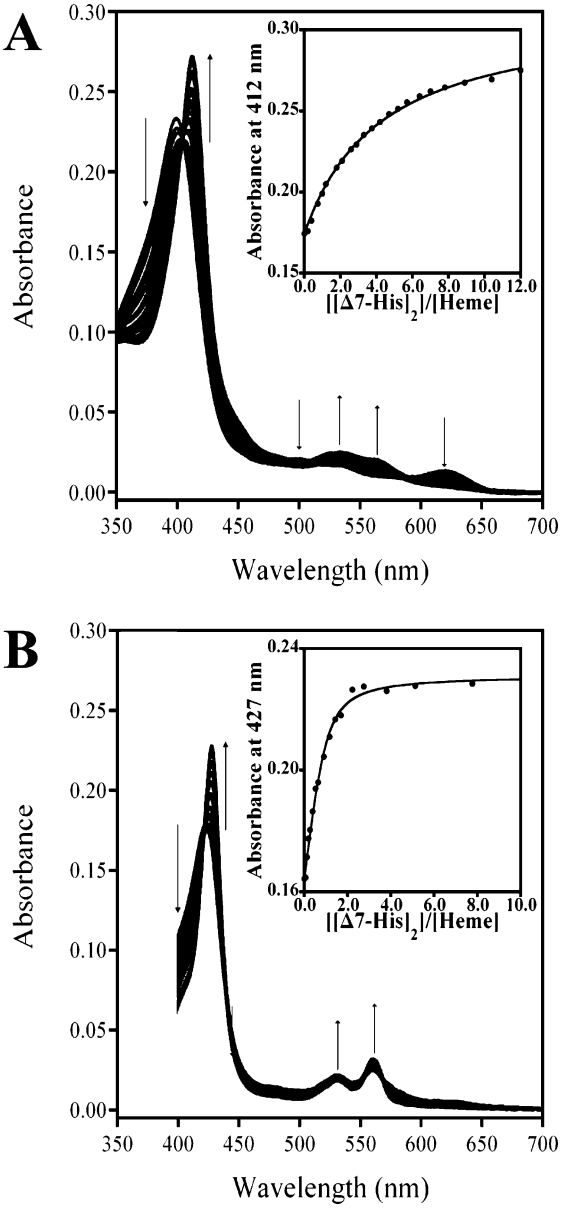

FIGURE 5: Representative competition titration of ferric (A) and ferrous (B) heme-loaded Dap1p with $[\Delta 7\text{-His}]_2$. The insets, which show the increase in absorption in the Soret band of heme-loaded $[\Delta 7\text{-His}]_2$, indicate the transfer of heme from Dap1p to $[\Delta 7\text{-His}]_2$; the change in absorption is fit to a competition model that gives the ferric and ferrous heme-loaded Dap1p K_D values.

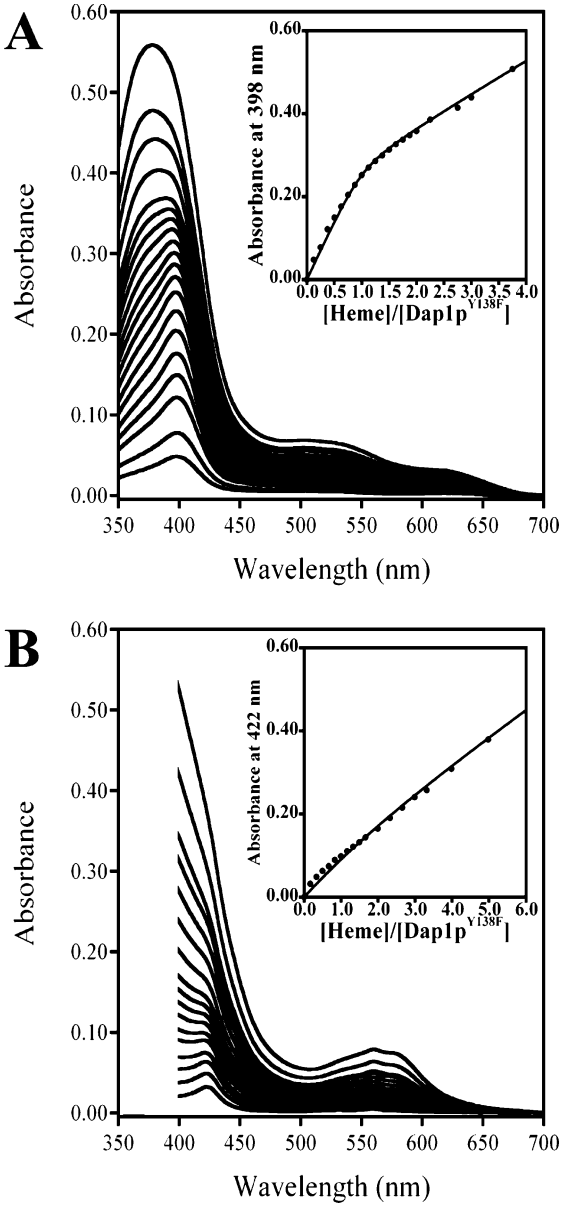

FIGURE 6: Direct titration of ferric (A) and ferrous (B) heme into Dap1p^{Y138F}. Insets show the change in absorption in the Soret bands as a result of heme binding and are fit to 1:1 binding models that give the ferric and ferrous K_D values of Dap1p^{Y138F}.

value is similar to the reduction potential of bovine catalase of −260 mV versus SHE, as well as other monotyrosinate heme proteins (*25*, *26*). Attempts to measure the reduction potential of *holo*-Dap1p^{Y138F} were thwarted by the extremely weak binding of ferrous heme to the mutant protein. However, since the reduction potential of a heme protein is determined by the relative stability of the ferric and ferrous heme states, the measured K_D values can be used to determine the reduction potential of the Dap1p^{Y138F} mutant (*27*). The 200 nM dissociation constant for ferric Dap1p^{Y138F} is 500-fold weaker than the 400 pM value of ferric holo-Dap1p. Using the thermodynamic relationship, $\Delta G = -RT \ln K_{eq}$, the 500-fold change in K_D represents a +3.7 kcal/mol destabilization of the ferric state Dap1p^{Y138F} relative to Dap1p. Since $\Delta E = \Delta\Delta G/nF$, the +3.7 kcal/mol destabilization of the ferric state should raise the midpoint potential +159 mV relative to Dap1p. The change in ferrous heme affinity also contributes to the reduction potential difference between these two proteins. The 5-fold, or 1 kcal/mol, destabilization of ferrous Dap1p^{Y138F} relative to Dap1p should lower the midpoint reduction potential of Dap1p^{Y138F} by 41 mV relative to Dap1p. Thus, the estimated reduction potential of Dap1p^{Y138F} is −189 mV (or −307 mV + 159 mV − 41 mV).

DISCUSSION

As discussed in the introduction, there is an ongoing debate in the literature regarding the biological role of yeast Dap1p. It has been proposed that Dap1p is involved in stabilizing protein levels of the P_{450} enzyme, Erg11p, principally because deletion of Dap1p from the genome did not affect the mRNA levels of Erg11p but did affect both the Erg11p protein level and sterol synthesis (*8*). This hypothesis, however, was brought into question when Hughes et al. observed that the

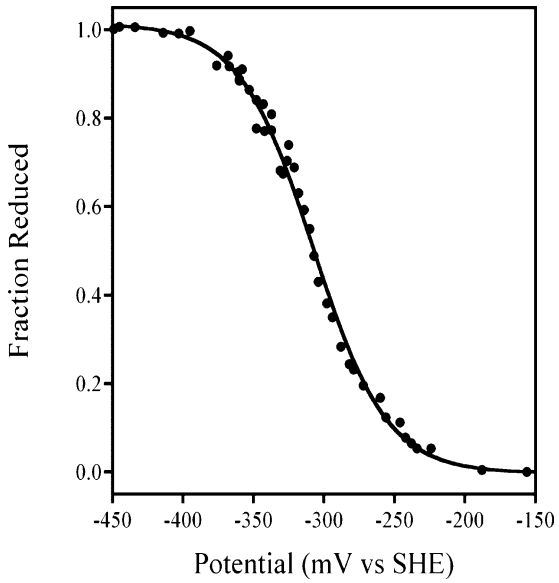

FIGURE 7: Redox potentiometry of heme-loaded Dap1p. The change in absorbance at the Soret as a function of solution potential is best fit to an $n = 1$ Nernst equation that gives a reduction potential of −307 mV vs SHE.

protein levels of the human homologue of Erg11p (Cyp51A1) were unaffected by the absence of the human homologue of Dap1p (PGRMC1). Additionally, they reported a 1:1 stoichiometric protein−protein interaction between Dap1p and Erg11p (protein homologues in both *S. pombe* and human cell lines) and found that *S. pombe dap1*Δ cells transformed with the low-affinity heme binding mutant, Dap1p^{Y138F}, also showed lowered sterol synthesis, suggesting that heme binding was important for the ability of Dap1p to rescue sterol synthesis (*9*).

In order to probe the role of heme binding and Dap1p function further, we embarked on a more detailed investigation of Dap1p. Initially, we probed the cellular properties of Erg11p and observed no change in mRNA or protein levels in the absence of genomic *DAP1* in *S. cerevisiae* (BY4741). This result is contradictory to that reported by Mallory, et al. (*8*), who used a different *S. cerevisiae* strain, but our data are consistent with the data of Hughes et al. and Crudden et al. for the human homologues which also showed no change in the P_{450} protein levels in the absence of PGRMC1 (*9*, *20*). In addition, we observed that the $t_{1/2}$ of Erg11p degradation was unchanged in the BY4741 *S. cerevisiae dap1*Δ strain. These results indicate that Dap1p does not stabilize Erg11p and weaken the case for Dap1p being a direct heme chaperone to Erg11p, as previously suggested (*6*−*8*).

Nevertheless, heme binding to Dap1p still appears to be required for ergosterol biosynthesis activity (*7*, *9*), and yet we previously reported that Dap1p, as isolated, contained only ∼30% bound heme (*7*). We resolved this inconsistency in the current investigation by achieving 80% ± 20% heme loading for Dap1p with direct titration of hemin chloride. This result indicated a tight affinity of the Dap1p for heme; however, the determination of the heme affinity to Dap1p (K_D) could not be determined by direct titration due to its tight K_D. HSM apomyoglobin was then titrated into Dap1p (30% heme-loaded) as a competitive substrate, and the K_D was approximated to be 100 fM by singular value decomposition (*15*). This method assumes that the K_D of HSM apomyoglobin, which has not been directly reported, is comparable to that of sperm whale myoglobin, the K_D of which is 10 fM (*16*, *17*). Having narrowed down the K_D range, Dap1p was titrated with $[\Delta 7\text{-His}]_2$, a well-characterized synthetic heme binding peptide (K_D of 160 pM), and the K_D of Dap1p was determined to be 400 ± 200 pM, with a 1:1 heme/protein ratio. This K_D value is smaller than that seen for a tyrosinate-ligated, heme transport protein (1.2 nM) (*28*) and smaller than that expected for a nonligated hydrophobic pocket in a hemoprotein (*29*). This data are supportive of Dap1p being a native hemoprotein, but not conclusive, since proteins such as BSA also have a strong affinity for ferric heme (250 pM) (*29*). The ferrous heme affinity of Dap1p ($K_D = 2 \pm 1\ \mu$M), however, is significantly weaker than that of ferric heme, which is consistent with expectations based on hard−soft acid−base theory for charged tyrosinate as the axial ligand (*30*). Our resonance Raman (RR) data (see the Supporting Information) on the ferrous−carbonyl complex support this conclusion, as axial ligands compete for σ-bond donation to the iron, and the high ν(Fe−CO) frequency observed in Dap1p is indicative of a weak trans ligand.

The reduction potential of Dap1p was measured to be −307 mV versus SHE which is comparable to the −260 mV value of bovine catalase, the axial ligand of which is also a tyrosinate (*25*, *26*). This value is in the range of cytochrome P_{450} reductases (*9*, *31*), making it tempting to suggest that Dap1p could provide electrons to Erg11p and hence increase the Erg11p activity in the cell with Dap1p present, as suggested by Hughes et al. (*9*). However, this hypothesis is unlikely since typical electron transport proteins, such as cytochrome b_5, have similar coordination environments between their biologically relevant oxidation states (*32*), and since the ferrous heme does not bind well to Dap1p, the heme would likely dissociate during redox cycling (*32*). Additionally, attempts to reduce the rat Dap1p homologue, IZA, by P_{450} reductases and cytochrome b_5 have been unsuccessful in vitro (*10*).

Previously, we proposed that Y138 was the axial ligand based on the fact that the as-isolated phenylalanine mutant, Dap1p^{Y138F} had no heme bound. We have subsequently been able to directly titrate Dap1p^{Y138F} with free heme and have observed a 1:1 ratio of protein to heme, with a K_D of 200 ± 100 nM. This affinity for heme is 500-fold weaker than that of Dap1p and is consistent with the loss of the native axial ligand, Y138 (*29*). The electronic spectrum of Dap1p^{Y138F} with heme bound, however, is remarkably similar to that of Dap1p. This result possibly indicates either a loosely coordinated solvent molecule or a substitute amino acid as the axial ligand. The latter hypothesis is possible since there are a number of potential anionic ligands in close proximity within the hydrophobic pocket, as seen in the NMR structure of the non-heme bound, homologue At2g24940.1 (*21*). Interestingly, the K_D of Dap1p^{Y138F} for ferrous heme ($K_D = 10\ \mu$M) is comparable to that of Dap1p ($K_D = 2\ \mu$M), supporting the hypothesis that the ferrous heme iron is not coordinated to a strong axial ligand and that the hydrophobic pocket is the primary determinant for ferrous heme binding for both wild-type Dap1p and Dap1p^{Y138F}.

The fact that Dap1p^{Y138F} still binds ferric heme with a relatively strong affinity inspired us to investigate the functional activity of this mutant protein. Hughes et al.

demonstrated that Dap1p^{Y138F} lowered sterol synthesis in *S. pombe* similar to that of the *dap1*Δ, (in both *S. pombe* and *S. cerevisiae* (*8*)) supporting the necessity of heme binding to Dap1p for Erg11p activation. They did not, however, demonstrate if Dap1p^{Y138F} could rescue the growth sensitivity of *dap1*Δ in the presence of MMS or fluconazole. We therefore expressed Dap1p^{Y138F} under the endogenous promoter in *dap1*Δ and found that Dap1p^{Y138F} did indeed rescue both phenotypes. On the face of it, this result contradicts the data of Hughes et al., suggesting that heme binding to Dap1p is not required for cellular activity. However, there are three possible interpretations that could explain this contradiction. First, it could be a simple difference in yeast strains if the function of Dap1p varies from species to species; our experiments were done in *S. cerevisiae*, whereas those of Hughes et al. were done in *S. pombe*. A second possibility is that Dap1p participates in several pathways and that the MMS and fluconazole sensitivities are unrelated to the lowered ergosterol production. Although there is a clear correlation between fluconazole and sterol toxicity (*33*), it is unclear exactly how DNA damage by MMS is related to sterol synthesis. A third, more likely explanation could be that the two Dap1p functional assays, the MMS/fluconazole lethality and sterol biosynthesis, have different sensitivities toward Dap1p function. For example, Hughes et al. showed that ergosterol biosynthesis in *S. pombe* with the Dap1p^{Y138F} mutant is lower than wild-type (*9*). However, the data also indicated that the level of the trienol and the toxic dienol (ergosta-5,7-dienol) mixture was lower in the Dap1p^{Y138F} strain than in the *dap1*Δ strain. Previously, Bard et al. demonstrated that deletion of Erg11p (or inhibition by fluconazole) led to the accumulation of the toxic dienol, which resulted in cell death for *S. cerevisiae* (*33*). However, deletion of both Erg11p and Erg3p abolished the accumulation of the dienol, which led to subsequent cell survival. Interestingly, it is unclear what level of dienol leads to cell sensitivity to fluconazole or MMS, since an LC_{50} titration has never been performed. Therefore, it is possible that Dap1p^{Y138F}, even with its lower heme affinity, has sufficient activity to lower the dienol level below the toxic limit, which then rescues the growth phenotypes. More investigations are clearly needed to distinguish between these three intriguing possibilities.

It should be noted that the growth sensitivity experiment with Dap1p^{D91G} showed no rescue, similar to that seen by Mallory et al. from *S. cerevisiae* and Crudden et al. from human cells (*8*, *20*). These results were previously explained as support for the hypothesis that heme binding was essential for Dap1p activity since the GST-Dap1p^{D91G} fusion protein did not bind heme. This may not be an appropriate conclusion since there is no evidence that GST-Dap1p^{D91G}, folds properly. Unfortunately, our attempts to express soluble Dap1p^{D91G} in *E. coli* and measure the heme K_D failed, possibly suggesting protein instability.

The proposed importance of heme binding for Dap1p appears in conflict with published data suggesting that MAPRs bind sterols (*1*, *3*, *21*, *34*, *35*). Reports of progesterone binding are predominantly with the porcine homologue PGRMC1, which was measured to have two binding affinities for progesterone, 11 and 286 nM (*1*). There is additional evidence for regulation of rat PGRMC1 (also known as Vema, IZA, 25-Dx, and sometimes mPR) by progesterone and involvement of PGRMC1 in cellular, nongenomic progesterone responses (*35*−*40*). However, progesterone binding by rat PGRMC1 was later shown to be nonspecific and weak by Min et al. (*6*). Instead, they found that rat PGRMC1 bound heme and activated the cytochrome P_{450} CYP21, a key enzyme of progesterone biosynthesis, in accordance with the biological function proposed by Hughes et al. (*9*). In addition, Dap1p isolated in *S. pombe* was shown to contain heme, although its percent incorporation was not measured (*9*). Together these data indicate that MAPRs do bind heme and interact with P_{450} enzymes in the cell, but it may also be possible that MAPRs have a dual function and bind sterols as well, possibly competitively with heme. More studies are needed to clarify the full biological role of MAPR proteins.

In summary, we have made several interesting contributions toward characterizing Dap1p's role as a heme binding protein. First, we have demonstrated that Dap1p in *S. cerevisiae* (BY4741) does not directly regulate Erg11p, be it mRNA, protein, or protein degradation. Second, Dap1p binds ferric heme tightly in a 1:1 stoichiometry (K_D = 400 pM) but ferrous heme poorly (K_D = 2 μM), supporting its designation as a ferric hemoprotein. Third, the RR results and the reduction potential of Dap1p are consistent with a five-coordinate heme iron with tyrosinate axial ligation (E = −307 mV). Finally, even though the weaker affinity of Dap1p^{Y138F} for ferric heme (K_D = 200 nM) lowers the production of ergosterol with respect to wild-type in *S. pombe*, the presence of Dap1p^{Y138F} is still sufficient to rescue the growth sensitivity of *dap1*Δ to fluconazole and MMS in *S. cerevisiae*. This result could potentially indicate that heme binding is not required for Dap1p activity; however, considering the preponderance of data mentioned above supporting heme binding to Dap1p, we consider this unlikely and have proposed three possible explanations. We are currently investigating these possibilities in the hope of defining the biological relationship between Dap1p and heme in greater detail.

ACKNOWLEDGMENT

We thank Zhu Zhiwu and Chris Vulpe for valuable discussions.

SUPPORTING INFORMATION AVAILABLE

Detailed explanation of the SVD method used to calculate the initial K_D value for Dap1p by competition with apomyoglobin and resonance Raman spectra. This material is available free of charge via the Internet at http://pubs.acs.org.

REFERENCES

1. Meyer, C., Schmid, R., Scriba, P. C., and Wehling, M. (1996) Purification and partial sequencing of high-affinity progesterone-binding site(s) from porcine liver membranes, *Eur. J. Biochem. 239*, 726−731.
2. Falkenstein, E., Meyer, C., Eisen, C., Scriba, P. C., and Wehling, M. (1996) Full-length cDNA sequence of a progesterone membrane-binding protein from porcine vascular smooth muscle cells, *Biochem. Biophys. Res. Commun. 229*, 86−89.
3. Falkenstein, E., Eisen, C., Schmieding, K., Krautkramer, M., Stein, C., Losel, R., and Wehling, M. (2001) Chemical modification and structural analysis of the progesterone membrane binding protein from porcine liver membranes, *Mol. Cell. Biochem. 218*, 71−79.
4. Selmin, O., Lucier, G. W., Clark, G. C., Tritscher, A. M., Vanden Heuvel, J. P., Gastel, J. A., Walker, N. J., Sutter, T. R., and Bell,

D. A. (1996) Isolation and characterization of a novel gene induced by 2,3,7,8-tetrachlorodibenzo-*p*-dioxin in rat liver, *Carcinogenesis 17*, 2609−2615.
5. Mifsud, W., and Bateman, A. (2002) Membrane-bound progesterone receptors contain a cytochrome b_5-like ligand-binding domain, *Genome Biol. 3*, 1−5.
6. Min, L., Strushkevich, N. V., Harnastai, I. N., Iwamoto, H., Gilep, A. A., Takemori, H., Usanov, S. A., Nonaka, Y., Hori, H., Vinson, G. P., and Okamoto, M. (2005) Molecular identification of adrenal inner zone antigen as a heme-binding protein, *FEBS J. 272*, 5832−5843.
7. Ghosh, K., Thompson, A. M., Goldbeck, R. A., Shi, X., Whitman, S., Oh, E., Zhiwu, Z., Vulpe, C., and Holman, T. R. (2005) Spectroscopic and biochemical characterization of heme binding to yeast Dap1p and mouse PGRMC1p, *Biochemistry 44*, 16729−16736.
8. Mallory, J. C., Crudden, G., Johnson, B. L., Mo, C., Pierson, C. A., Bard, M., and Craven, R. J. (2005) Dap1p, a heme-binding protein that regulates the cytochrome P_{450} protein Erg11p/Cyp51p in *Saccharomyces cerevisiae*, *Mol. Cell. Biol. 25*, 1669−1679.
9. Hughes, A. L., Powell, D. W., Bard, M., Eckstein, J., Barbuch, R., Link, A. J., and Espenshade, P. J. (2007) Dap1/PGRMC1 binds and regulates cytochrome P_{450} enzymes, *Cell Metab. 5*, 143−149.
10. Min, L., Takemori, H., Nonaka, Y., Katoh, Y., Doi, J., Horike, N., Osamu, H., Raza, F. S., Vinson, G. P., and Okamoto, M. (2004) Characterization of the adrenal-specific antigen IZA (inner zone antigen) and its role in the steroidogenesis, *Mol. Cell. Endocrinol. 215*, 143−148.
11. Hand, R. A., Jia, N., Bard, M., and Craven, R. J. (2003) *Saccharomyces cerevisiae* Dap1p, a novel DNA damage response protein related to the mammalian membrane-associated progesterone receptor, *Eukaryotic Cell 2*, 306−317.
12. Ooi, C. E., Rabinovich, E., Dancis, A., Bonifacino, J. S., and Klausner, R. D. (1996) Copper-dependent degradation of the *Saccharomyces cerevisiae* plasma membrane copper transporter Ctr1p in the apparent absence of endocytosis, *EMBO J. 15*, 3515−3523.
13. Padmanabhan, S., Marqusee, S., Ridgeway, T., Laue, T. M., and Baldwin, R. L. (1990) Relative helix-forming tendencies of nonpolar amino acids, *Nature 344*, 268−270.
14. Berry, E. A., and Trumpower, B. L. (1987) Simultaneous determination of hemes a, b, and c from pyridine hemochrome spectra, *Anal. Biochem. 161*, 1−15.
15. Hendler, R. W., and Shrager, R. I. (1994) Deconvolutions based on singular value decomposition and the pseudoinverse: a guide for beginners, *J. Biochem. Biophys. Methods 28*, 1−33.
16. Hargrove, M. S., and Olson, J. S. (1996) The stability of holomyoglobin is determined by heme affinity, *Biochemistry 35*, 11310−11318.
17. Hargrove, M. S., Wilkinson, A. J., and Olson, J. S. (1996) Structural factors governing hemin dissociation from metmyoglobin, *Biochemistry 35*, 11300−11309.
18. Reddi, A. R., Reedy, C. J., Mui, S., and Gibney, B. R. (2007) Thermodynamic investigation into the mechanisms of proton-coupled electron transfer events in heme protein maquettes, *Biochemistry 46*, 291−305.
19. Dutton, P. L. (1978) Redox potentiometry: determination of midpoint potentials of oxidation−reduction components of biological electron-transfer systems, *Methods Enzymol. 54*, 411−435.
20. Crudden, G., Chitti, R. E., and Craven, R. J. (2005) Hpr6 (heme-1 domain protein) regulates the susceptibility of cancer cells to chemotherapeutic drugs, *J. Pharmacol. Exp. Ther. 316*, 448−455.
21. Song, J., Vinarov, D., Tyler, E. M., Shahan, M. N., Tyler, R. C., and Markley, J. L. (2004) Hypothetical protein At2g24940.1 from *Arabidopsis thaliana* has a cytochrome b_5 like fold, *J. Biomol. NMR 30*, 215−218.
22. Fronticelli, C., and Bucci, E. (1963) Acetone extraction of heme from myoglobin and hemoglobin at acid pH, *Biochim. Biophys. Acta 78*, 530−531.
23. Teale, F. W. J. (1959) Cleavage of the haem-protein link by acid methylethylketone, *Biochim. Biophys. Acta 35*, 543.
24. Reedy, C. J., Kennedy, M. L., and Gibney, B. R. (2003) Thermodynamic characterization of ferric and ferrous haem binding to a designed four-alpha-helix protein, *Chem. Commun. (Cambridge, U.K.)*, 570−571.
25. Wang, L., Wang, J., and Zhou, F. (2004) Direct electrochemistry of catalase at a gold electrode modified with single-wall carbon nanotubes, *Electroanalysis 16*, 627−632.
26. Hildebrand, D. P., Burk, D. L., Maurus, R., Ferrer, J. C., Brayer, G. D., and Mauk, A. G. (1995) The proximal ligand variant His93Tyr of horse heart myoglobin, *Biochemistry 34*, 1997−2005.
27. Reedy, C. J., and Gibney, B. R. (2004) Heme protein assemblies, *Chem. Rev. 104*, 617−649.
28. Tong, Y., and Guo, M. (2007) Cloning and characterization of a novel periplasmic heme-transport protein from the human pathogen *Pseudomonas aeruginosa*, *J. Biol. Inorg. Chem. 12*, 735−750.
29. Hargrove, M. S., Barrick, D., and Olson, J. S. (1996) The association rate constant for heme binding to globin is independent of protein structure, *Biochemistry 35*, 11293−11299.
30. Pearson, R. G. (1963) Hard and soft acids and bases, *J. Am. Chem. Soc. 85*, 3533−3539.
31. Munro, A. W., Noble, M. A., Robledo, L., Daff, S. N., and Chapman, S. K. (2001) Determination of the redox properties of human NADPH-cytochrome P_{450} reductase, *Biochemistry 40*, 1956−1963.
32. Gray, H. B., and Winkler, J. R. (2004) Electron tunneling through proteins, *Q. Rev. Biophys. 36*, 341−372.
33. Bard, M., Lees, N. D., Turi, T., Craft, D., Cofrin, L., Barbuch, R., Koegel, C., and Loper, J. C. (1993) Sterol synthesis and viability of erg11 (cytochrome P_{450} lanosterol demethylase) mutations in *Saccharomyces cerevisiae* and *Candida albicans*, *Lipids 28*, 963−967.
34. Losel, R., Dorn-Beineke, A., Falkenstein, E., Wehling, M., and Feuring, M. (2004) Porcine spermatozoa contain more than one membrane progesterone receptor, *Int. J. Biochem. Cell Biol. 36*, 1532−1541.
35. Falkenstein, E., Heck, M., Gerdes, D., Grube, D., Christ, M., Weigel, M., Buddhikot, M., Meizel, S., and Wehling, M. (1999) Specific progesterone binding to a membrane protein and related nongenomic effects on Ca^{2+}-fluxes in sperm, *Endocrinology 140*, 5999−6002.
36. Labombarda, F., Gonzalez, S. L., Deniselle, M. C., Vinson, G. P., Schumacher, M., De Nicola, A. F., and Guennoun, R. (2003) Effects of injury and progesterone treatment on progesterone receptor and progesterone binding protein 25-Dx expression in the rat spinal cord, *J. Neurochem. 87*, 902−913.
37. Peluso, J. J. (2007) Non-genomic actions of progesterone in the normal and neoplastic mammalian ovary, *Semin. Reprod. Med. 25*, 198−207.
38. Peluso, J. J., Pappalardo, A., Losel, R., and Wehling, M. (2006) Progesterone membrane receptor component 1 expression in the immature rat ovary and its role in mediating progesterone's antiapoptotic action, *Endocrinology 147*, 3133−3140.
39. Gonzalez, S. L., Labombarda, F., Deniselle, M. C., Mougel, A., Guennoun, R., Schumacher, M., and De Nicola, A. F. (2005) Progesterone neuroprotection in spinal cord trauma involves up-regulation of brain-derived neurotrophic factor in motoneurons, *J. Steroid Biochem. Mol. Biol. 94*, 143−149.
40. Krebs, C. J., Jarvis, E. D., Chan, J., Lydon, J. P., Ogawa, S., and Pfaff, D. W. (2000) A membrane-associated progesterone-binding protein, 25-Dx, is regulated by progesterone in brain regions involved in female reproductive behaviors, *Proc. Natl. Acad. Sci. U.S.A. 97*, 12816−12821.

BI7013739